

Privacy Protection Against Personalized Text-to-Image Synthesis via Cross-image Consistency Constraints

GUANYU WANG, Beihang University, China

KAILONG WANG, Huazhong University of Science and Technology, China

YIHAO HUANG, Nanyang Technological University, Singapore

MINGYI ZHOU, Beihang University, China

ZHANG QING CNWATCHER, ByteDance, China

GE GUANG PU, East China Normal University, China

LI LI, Beihang University, China

The rapid advancement of diffusion models and personalization techniques has made it possible to recreate individual portraits from just a few publicly available images. While such capabilities empower various creative applications, they also introduce serious privacy concerns, as adversaries can exploit them to generate highly realistic impersonations. To counter these threats, anti-personalization methods have been proposed, which add adversarial perturbations to published images to disrupt the training of personalization models. However, existing approaches largely overlook the intrinsic multi-image nature of personalization and instead adopt a naive strategy of applying perturbations independently, as commonly done in single-image settings. This neglects the opportunity to leverage inter-image relationships for stronger privacy protection. Therefore, we advocate for a group-level perspective on privacy protection against personalization. Specifically, we introduce Cross-image Anti-Personalization (CAP), a novel framework that enhances resistance to personalization by enforcing style consistency across perturbed images. Furthermore, we develop a dynamic ratio adjustment strategy that adaptively balances the impact of the consistency loss throughout the attack iterations. Extensive experiments on the classical CelebHQ and VGGFace2 benchmarks show that CAP substantially improves existing methods.

ACM Reference Format:

Guanyu Wang, Kailong Wang, Yihao Huang, Mingyi Zhou, Zhang Qing cnwatcher, Geguang Pu, and Li Li. 2025. Privacy Protection Against Personalized Text-to-Image Synthesis via Cross-image Consistency Constraints. 1, 1 (April 2025), 15 pages. <https://doi.org/10.1145/nnnnnnn.nnnnnnn>

1 Introduction

With the rapid advancement and widespread adoption of Diffusion Models (DMs) [8], personalization techniques—also known as customization—such as DreamBooth [16] and Textual Inversion [4] have enabled users to fine-tune generative models using only a handful of example images. These methods make it possible to faithfully replicate specific objects, artistic styles, and even individual portraits. While personalization has demonstrated remarkable potential in areas such as artistic creation, virtual character design, and digital content generation [23, 26, 27], it also introduces serious

Authors' Contact Information: Guanyu Wang, Beihang University, China; Kailong Wang, Huazhong University of Science and Technology, China; Yihao Huang, Nanyang Technological University, Singapore; Mingyi Zhou, Beihang University, China; Zhang Qing cnwatcher, ByteDance, China; Geguang Pu, East China Normal University, China; Li Li, Beihang University, China.

Permission to make digital or hard copies of all or part of this work for personal or classroom use is granted without fee provided that copies are not made or distributed for profit or commercial advantage and that copies bear this notice and the full citation on the first page. Copyrights for components of this work owned by others than the author(s) must be honored. Abstracting with credit is permitted. To copy otherwise, or republish, to post on servers or to redistribute to lists, requires prior specific permission and/or a fee. Request permissions from permissions@acm.org.

© 2025 Copyright held by the owner/author(s). Publication rights licensed to ACM.

Manuscript submitted to ACM

Manuscript submitted to ACM

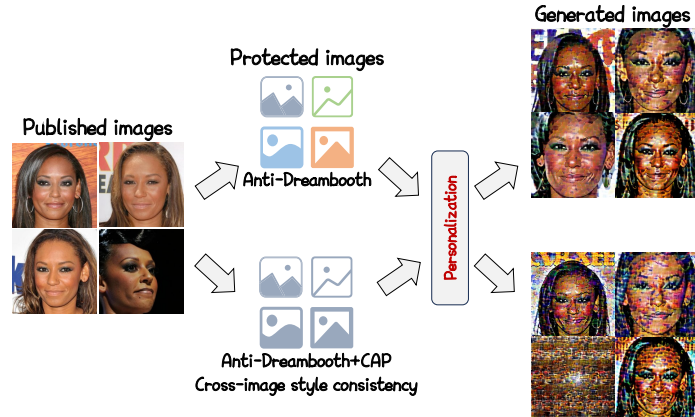


Fig. 1. Comparison between Anti-DreamBooth before and after adding our CAP method. Our method further boosts its ability to de-identify. The core idea is to encourage the cross-image consistency when generating protected images.

concerns related to privacy and intellectual property protection. In particular, adversaries can misuse these techniques to reconstruct the likeness of a real individual with high fidelity, facilitating malicious activities such as misinformation campaigns, identity theft, and synthetic content forgery. Such misuse poses substantial threats to personal privacy and societal trust in digital media.

To safeguard personal privacy from potential misuse by malicious actors, a widely adopted strategy is to inject adversarial noise into target images to be protected images, thereby misleading personalization models into learning incorrect identity representations. Note that in this paper, protected images and perturbed images refer to the same set of adversarially modified images. Representative methods in this direction include Anti-DreamBooth [22] and SimAC [24]. Anti-DreamBooth defends against unauthorized personalization by maximizing the reconstruction loss of a surrogate model to hinder identity learning. SimAC extends this approach with diffusion-specific enhancements, accounting for perceptual variations across denoising steps and the statistics of intermediate features, leading to better privacy protection.

A common limitation of existing privacy protection methods lies in their image-wise design paradigm: **they apply adversarial perturbations to each image independently, without considering inter-image relationships**. While effective in single-image tasks, this approach fails to reflect the intrinsic nature of personalization, which is trained over a set of images to form a unified identity representation. We argue that defending against such threats requires a group-level perspective. By explicitly modeling relationship across perturbed images, it becomes possible to disrupt the personalization more effectively, thereby strengthening privacy protection.

Building on this group-level perspective, we propose a novel method called **Cross-image Anti-Personalization**, termed CAP. Unlike existing approaches such as Anti-DreamBooth and SimAC that primarily rely on reconstruction loss, CAP introduces an additional consistency loss that promotes style uniformity across perturbed images by aligning their Gram matrices. To effectively balance the contributions of reconstruction and consistency losses, we further propose a dynamic ratio adjustment strategy that adaptively balances the impact of the consistency loss throughout the attack iterations. Extensive experiments on the Celeb-HQ [9] and VGGFace2 [1] datasets validate the effectiveness of CAP in preserving privacy against personalization.

To sum up, our work has the following contributions:

- To the best of our knowledge, this is the first work to reframe anti-personalization as a cross-image privacy protection task by explicitly modeling inter-image consistency.
- We propose the CAP method, which incorporates a style-based consistency loss to encourage perturbed images to share similar style representations, along with a dynamic ratio adjustment strategy that adaptively balances its contribution during optimization. This method can be directly integrated into existing anti-personalization approaches to enhance their privacy protection performance.
- Extensive experiments on two standard benchmark datasets validate the effectiveness of the proposed CAP method.

2 Related Work

2.1 Text-to-Image Generation Models

With the emergence of large-scale datasets such as LAION-5B [17], text-to-image (T2I) generative models have witnessed rapid advancements, unlocking new possibilities across a wide range of visual applications and drawing significant public attention.

Among various text-to-image frameworks, Variational Autoencoders (VAEs) [10] often suffer from low sample quality, while Generative Adversarial Networks (GANs) [6] produce sharper images but are prone to training instability. In contrast, Diffusion Models (DMs) [8] leverage a gradual denoising process by iteratively adding and removing noise, achieving notable improvements in image fidelity and training stability. Despite their strengths, diffusion-based T2I models are computationally intensive and heavily reliant on large-scale training data [17]. To address this, Stable Diffusion (SD) [20] was introduced, based on Latent Diffusion Models (LDMs) [15], which shift the generative process to a compressed latent space—greatly reducing resource requirements while enabling high-resolution image synthesis.

2.2 Personalization

Personalization [4, 11, 16] in text-to-image generation aims to adapt pre-trained models to capture user-specific concepts. This is typically achieved by fine-tuning a diffusion model with a small set of subject images (usually 3–5) and associating them with a unique identifier token (e.g., “a *sks* person”), enabling the model to synthesize the subject in diverse, unseen contexts while preserving its core visual characteristics.

DreamBooth [16] and Textual Inversion [4] are two representative approaches. DreamBooth fine-tunes the entire model using a few subject images and an identifier token, allowing for high-fidelity generation in novel scenes, but at the cost of increased computational overhead and potential degradation of the model’s general knowledge. In contrast, Textual Inversion preserves the model weights and instead learns a new word embedding to represent the subject. While more efficient, it struggles with expressiveness, particularly for complex visual concepts. Building on these methods, subsequent work such as Custom-Diffusion [11] explores hybrid and more efficient personalization strategies.

Despite their impressive capabilities, these personalization techniques raise serious privacy concerns. Because they can extract and reproduce identifiable features—such as a person’s face—from only a few input images, they enable unauthorized identity cloning. In scenarios where personal photos are scraped or leaked, such methods can be exploited to generate realistic, unauthorized images of individuals, posing significant threats to privacy and consent.

2.3 Privacy Protection against Personalization

As AI models continue to advance, concerns over their potential misuse, such as identity theft, impersonation, and unauthorized fine-tuning, have grown significantly [13, 22, 28]. In response, recent research has shifted from passive defenses to proactive strategies that aim to prevent such exploitation at the data level.

In particular, the rise of diffusion-based personalization methods [4, 11, 16] has sparked growing interest in privacy protection techniques tailored to these models. To mitigate risks such as identity leakage, unauthorized mimicry, and malicious fine-tuning, researchers have proposed several privacy-preserving perturbation methods [12, 22, 24] that subtly modify user-provided images. These perturbations reduce the effectiveness of downstream personalization, offering a robust form of privacy protection.

For example, Anti-DreamBooth [22] introduces the first data-side defense against personalization by generating adversarial perturbations that distort the identity concept learned during fine-tuning, resulting in failed or incoherent generations. Building on this, SimAC [24] enhances protection by adaptively injecting perturbations at the most vulnerable timesteps of the diffusion process. It also incorporates a feature interference loss to further disrupt identity learning, achieving stronger protection with minimal visual distortion. SimAC is the state-of-the-art privacy protection method against personalization.

Although existing methods offer promising protection, they treat each image independently, ignoring that personalization is a multi-image task. This neglect of inter-image relationships limits their ability to disrupt the model’s learning of shared identity or style representations.

2.4 Style Transfer

Style transfer aims to generate an image that preserves the content of one image while adopting the visual style of another. A seminal work by Gatys et al. [5] formulates this task as an optimization problem over a pre-trained convolutional neural network (CNN). In their approach, content is captured using feature activations from deeper layers of the CNN, while style is represented via the Gram matrices of feature maps from multiple layers. By simultaneously minimizing the difference between the target image’s content features and those of the source content image, and aligning its style features with those of the reference style image, the method produces a visually coherent and stylized result.

3 Preliminary

Diffusion models are a type of generative models [8] that decompose the data generation process into two complementary stages: a forward process and a reverse (backward) process. In the forward process, noise is gradually added to the input image, transforming the original data distribution into a standard Gaussian noise. Conversely, the reverse process is trained to recover the original data from pure noise by learning to invert this corruption process.

Given an input image x_0 , the forward process perturbs the data using a predefined noise schedule $\{\beta^t : \beta^t \in (0, 1)\}_{t=1}^T$, which controls the magnitude of noise added over T steps. This results in a sequence of noisy latent variables $\{x^1, x^2, \dots, x^T\}$. At each timestep t , the noisy sample x^t is generated as:

$$x^t = \sqrt{\alpha^t} x_0 + \sqrt{1 - \alpha^t} \epsilon, \quad (1)$$

where $\alpha^t = 1 - \beta^t$, $\bar{\alpha}^t = \prod_{s=1}^t \alpha^s$, and $\epsilon \sim \mathcal{N}(0, \mathbf{I})$ represents standard Gaussian noise.

The reverse process aims to denoise x^{t+1} to obtain a less noisy x^t by estimating the noise component ϵ using a neural network $\epsilon_\theta(x^{t+1}, t)$. The model is trained to minimize the ℓ_2 distance between the true noise and the predicted noise:

$$\mathcal{L}_{\text{uncondition}}(\epsilon_\theta, x_0) = \mathbb{E}_{x_0, t, \epsilon \sim \mathcal{N}(0,1)} \|\epsilon - \epsilon_\theta(x^{t+1}, t)\|_2^2, \quad (2)$$

where t is uniformly sampled from $\{1, \dots, T\}$.

Conditional Diffusion Models. In contrast to unconditional diffusion models, conditional (prompt-based) diffusion models guide the generation process using an additional condition or prompt c . This enables the model to produce photorealistic outputs that are semantically aligned with the given text prompt or concept. The training objective is then extended as:

$$\mathcal{L}_{\text{cond}}(\epsilon_\theta, x_0, c) = \mathbb{E}_{x_0, t, \epsilon \sim \mathcal{N}(0,1)} \|\epsilon - \epsilon_\theta(x^{t+1}, t, c)\|_2^2. \quad (3)$$

Note that in this paper, the condition prompt is the concept \mathcal{S} .

Adversarial attacks. Since anti-personalization methods use adversarial perturbations on published images to resist personalization, we first briefly review adversarial attacks. These attacks aim to add subtle noise that misleads models, typically studied in classification settings. Given a model f and an input image x , an adversarial example x' is generated such that it remains visually indistinguishable from x , yet induces a misclassification, i.e., $y_{\text{true}} \neq f(x')$. To ensure the perturbation is imperceptible, it is typically constrained within an η -ball under an ℓ_p norm, i.e., $\|x' - x\|_p \leq \eta$. The optimal perturbation is obtained by maximizing the classification loss under the true label:

$$\delta_{\text{adv}} = \arg \max_{\|\delta\|_p \leq \eta} \mathcal{L}(f(x + \delta), y_{\text{true}}), \quad (4)$$

Projected Gradient Descent (PGD) [14] is one of the most widely used methods to generate such adversarial examples. It adopts an iterative optimization process with K iterations, where the adversarial example x' is updated as follows:

$$x'_0 = x, x'_k = \Pi_{(x, \eta)} \left(x'_{k-1} + \alpha \cdot \text{sgn} \left(\nabla_x \mathcal{L}(f(x'_{k-1}), y_{\text{true}}) \right) \right) \quad (5)$$

Here, $\Pi_{x, \eta}(z)$ denotes the projection operator that ensures the perturbed image z stays within the η -ball centered at the original image x . The final adversarial example x'_K is obtained after a fixed number (K) of iterations.

4 Methodology

4.1 Problem Formulation

Personalization, as a powerful tool for generating photo-realistic outputs of a target instance, can be a double-edged sword. When misused, it may produce harmful images targeting specific individuals. To mitigate this risk, existing privacy protection methods introduce adversarial perturbations to each user's image. These perturbations are designed to disrupt the concept learned by personalized models, resulting in generated images that contain noticeable artifacts. We formally define the problem below.

Given a set of facial images $\mathcal{X} = \{x_i\}_{i=1}^N$ corresponding to a target individual and a text-to-image (T2I) model ϵ_θ , a personalization method $\mathcal{P}(\cdot, \cdot)$ can learn an identity-specific concept $\mathcal{S}_o = \mathcal{P}(\epsilon_\theta, \mathcal{X})$, where \mathcal{S}_o is typically represented as a token. The learned concept can be used to generate images resembling the target individual via $\epsilon_\theta(\mathcal{S}_o)$. The privacy protection task seeks to degrade the quality of the learned concept by modifying the input image set \mathcal{X} .

Specifically, for each image $x_i \in \mathcal{X}$, an adversarial perturbation δ_i is added on it to obtain a perturbed image $x'_i = x_i + \delta_i$, forming the protected dataset $\mathcal{X}' = \{x'_i\}_{i=1}^N$. Only the perturbed images are made publicly available, i.e., \mathcal{X}' is released while the original \mathcal{X} remains private. An adversary can collect \mathcal{X}' and attempt to learn a identity

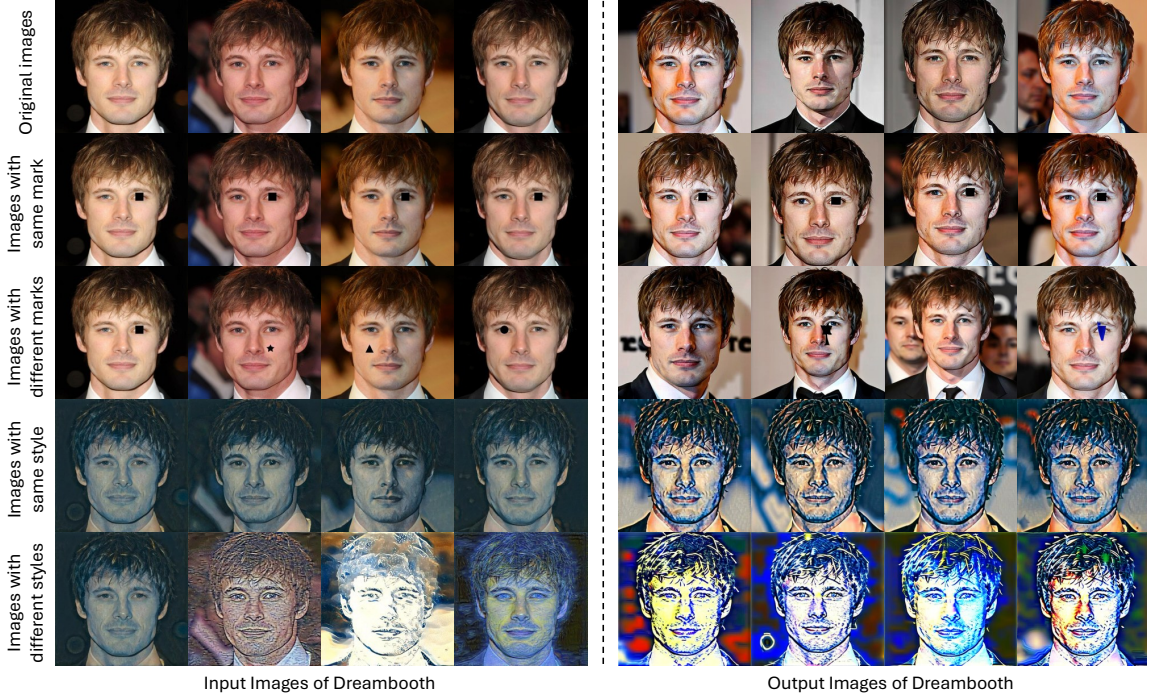


Fig. 2. Motivation. The first row presents the original input images. The second and third rows display perturbed images with consistent and inconsistent disruption marks, respectively. The fourth and fifth rows show images modified to share the same style or different styles. The first four columns are input images used for personalization, and the last four are samples generated using the learned identity concept.

concept $\mathcal{S}' = \mathcal{P}(\epsilon_\theta, \mathcal{X}')$, where \mathcal{P} is the personalization method. The goal of adversarial protection is to optimize the perturbation set $\Delta = \{\delta_i\}_{i=1}^N$ such that the images generated from \mathcal{S}' contain noticeable artifacts and deviate from the identity in \mathcal{X} . Formally, this can be expressed as:

$$\Delta^* = \arg \min_{\Delta} \mathcal{A}(\epsilon_\theta(\mathcal{S}'), \mathcal{X}) \quad (6)$$

$$\text{s.t. } \mathcal{S}' = \arg \min_{\mathcal{S}} \sum_{i=1}^N \mathcal{L}_{\mathcal{P}}(\epsilon_\theta, x_i + \delta_i, \mathcal{S}), \quad (7)$$

$$\text{and } \|\delta_i\|_p \leq \eta, \quad \forall i \in \{1, 2, \dots, N\}. \quad (8)$$

Here, $\mathcal{A}(\cdot, \cdot)$ denotes an evaluation function that assesses (1) the quality of images $\epsilon_\theta(\mathcal{S}')$ and (2) the identity consistency between the generated images and the reference images \mathcal{X} . Lower $\mathcal{A}(\cdot, \cdot)$ means worse quality of concept \mathcal{S}' . $\mathcal{L}_{\mathcal{P}}(\cdot, \cdot, \cdot)$ is the loss function used in personalization to learn the concept from the input images. η denotes the strength of the adversarial perturbation.

4.2 Motivation

Existing privacy protection methods (e.g., Anti-DreamBooth [22], SimAC [24]) realize the privacy protection by maximizing the reconstruction error (i.e., \mathcal{L}_{cond} (Eq. (3))) of clean images with concept \mathcal{S} as input prompt. Specifically,

the reconstruction loss is:

$$\mathcal{L}_{re} = \sum_{i=1}^N \mathcal{L}_{cond}(\epsilon_{\theta}, x_i, \mathcal{S}^*), \quad (9)$$

$$\text{s.t. } \mathcal{S}^* = \arg \min_{\mathcal{S}} \sum_{i=1}^N \mathcal{L}_{\mathcal{P}}(\epsilon_{\theta}, x_i + \delta_i, \mathcal{S}), \quad (10)$$

$$\text{and } \|\delta_i\|_p \leq \eta, \quad \forall i \in \{1, 2, \dots, N\}, \quad (11)$$

Despite their demonstrated effectiveness, these protection methods share the same limitation.

Limitation of existing method. Anti-personalization aims to prevent text-to-image models from learning the identity of a specific individual by introducing adversarial perturbations to a set of their images. Unlike traditional adversarial attacks in single-image tasks such as classification, which require only a single perturbed sample, anti-personalization involves generating multiple perturbed images of the same subject. This fundamental distinction underscores the importance of modeling the relationships among these samples to ensure effective identity obfuscation.

However, existing privacy protection methods often overlook this aspect by optimizing each adversarial perturbation independently, without explicitly enforcing consistency across the perturbed images. This is problematic because personalization methods are inherently designed to extract shared semantic features across multiple images to construct a coherent identity representation, rather than learning the concept from a single image alone.

High-level idea. Therefore, we argue that a more effective anti-personalization strategy should move beyond isolated perturbations and instead incorporate inter-sample relationships into the optimization process. By disrupting the consistency that personalization methods rely on, this approach can provide stronger privacy protection against personalization.

To support this intuition, we conduct a preliminary experiment using DreamBooth. As shown in Figure 2, the first row presents the original input images. The second and third rows display perturbed images with consistent and inconsistent disruption marks, respectively. The fourth and fifth rows show images modified to share the same style or different styles. The first four columns are input images used for personalization, and the last four are samples generated using the learned identity concept.

In the second row, where all input images share the same disruption mark, this pattern is consistently reflected in the generated results. In contrast, when each image contains a different disruption mark, as shown in the third row, none of the patterns appear in the outputs. A similar effect is observed in the fourth and fifth rows. When the input images share the same style, it is preserved in the generated results. When the styles differ, no consistent style is learned. These results suggest that personalization models tend to encode cross-image consistency, whether adversarial or stylistic, into the learned identity representation.

Overall, these findings highlight the importance of cross-image consistency modeling. Introducing diversity across perturbed samples, or explicitly controlling their consistency, can enhance the effectiveness of anti-personalization by disrupting the coherent patterns that personalization models seek to exploit.

Inspired by the observation that personalization models are inherently designed to extract commonalities across multiple input images, we propose that if the input set contains both shared semantic content A (e.g., a person’s identity) and an additional consistent signal B (e.g., a noise pattern), the model is likely to encode both into the learned concept, resulting in $\mathcal{S}^* \approx A + B$. Since the model lacks the ability to differentiate between genuine identity features

Algorithm 1: Algorithm

Input: published clean images \mathcal{X} , attack iteration steps K , start step of adding consistency loss \hat{k} , step length α , search ratio range $[0, R]$, denoising model ϵ_θ and condition prompt \mathcal{S} .

Output: protected images \mathcal{X}'^K .

```

1  $\mathcal{X}'^1 \leftarrow \mathcal{X}$ ;
2 for  $k = 1$  to  $K$  do
3    $\mathcal{L}_{re}^k \leftarrow \sum_{i=1}^N \mathcal{L}_{cond}(\epsilon_\theta, x_i'^k, \mathcal{S})$ ;
4   if  $k < \hat{k}$  then
5      $\mathcal{X}'^{k+1} \leftarrow \mathcal{X}'^k + \alpha \cdot \text{sign}(\nabla \mathcal{L}_{re}^k)$ ;
6   else
7      $\mathcal{L}_{consistency}^k \leftarrow \frac{1}{N} \sum_{i=1}^N \|G^l(x_i'^k) - \bar{G}^l\|_2^2$ ;
8      $\lambda \leftarrow 0$ ;
9      $\mathcal{L}_{max} \leftarrow 0$ ;
10    for  $r = 0$  to  $R$  do
11       $\mathcal{L}^{k,r} \leftarrow \mathcal{L}_{re}^k + r * \mathcal{L}_{consistency}^k$ ;
12       $\mathcal{X}'^{k,r} \leftarrow \mathcal{X}'^k + \alpha \cdot \text{sign}(\nabla \mathcal{L}^{k,r})$ ;
13       $\mathcal{L}_{re}^{k,r} \leftarrow \sum_{i=1}^N \mathcal{L}_{cond}(\epsilon_\theta, x_i'^{k,r}, \mathcal{S})$ ;
14      if  $\mathcal{L}_{re}^{k,r} > \mathcal{L}_{max}$  then
15         $\mathcal{L}_{max} \leftarrow \mathcal{L}_{re}^{k,r}$ ;
16         $\lambda \leftarrow r$ ;
17       $\mathcal{L}^k \leftarrow \mathcal{L}_{re}^k + \lambda * \mathcal{L}_{consistency}^k$ ;
18       $\mathcal{X}'^{k+1} \leftarrow \mathcal{X}'^k + \alpha \cdot \text{sign}(\nabla \mathcal{L}^k)$ ;
19 return  $\mathcal{X}'^K$ ;
```

and consistent noise, it treats both as integral parts of the identity. As a result, images generated from this concept tend to consistently exhibit the noise signal as a noticeable artifact.

4.3 Method Overview

To construct a privacy protection method against personalization while considering the inter-sample relationships between perturbed images, we propose the method with a specifically designed loss.

Relationship design. To model the relationship among the perturbed input images, we leverage the Gram matrix [19], a widely used representation for capturing image style and texture. Given a set of perturbed images \mathcal{X}' , we extract their deep feature representations using a pre-trained convolutional neural network (e.g., VGG-19 [18]) at a certain layer l , denoted as $f^l(x'_i) \in \mathbb{R}^{C \times HW}$, where C is the number of channels, and H, W are the height and width of the images. The Gram matrix for each image at layer l is:

$$G^l(x'_i) = f^l(x'_i) \cdot (f^l(x'_i))^\top \quad (12)$$

This matrix captures the pairwise correlations between feature channels and reflects the image's style information. To measure the similarity between two perturbed images x'_i and x'_j , we compute the difference between their Gram matrices:

$$\text{Sim}_{ij}^l = \left\| G^l(x'_i) - G^l(x'_j) \right\|_2^2 \quad (13)$$

A smaller Sim_{ij}^l indicates more similar styles between x'_i and x'_j .

Loss design. To inject interference into the concept learned by the personalization method across perturbed inputs, we propose a *consistency loss* that enforces stylistic similarity among the images. Instead of computing pairwise distances, we first calculate the mean Gram matrix across all perturbed images as the reference style:

$$\bar{G}^l = \frac{1}{N} \sum_{i=1}^N G^l(x'_i) \quad (14)$$

Then, we measure the discrepancy between each image’s Gram matrix and the mean style representation. The consistency loss is:

$$\mathcal{L}_{\text{consistency}} = \frac{1}{N} \sum_{i=1}^N \left\| G^l(x'_i) - \bar{G}^l \right\|_2^2 \quad (15)$$

Minimizing this loss encourages all perturbed images to exhibit a unified style in the feature space, which promotes coherent interference against the identity-specific features that personalization methods attempt to capture.

To sum up, the final loss used in our method is \mathcal{L} ,

$$\mathcal{L} = \mathcal{L}_{re} + \lambda * \mathcal{L}_{\text{consistency}}, \quad (16)$$

where λ is the ratio used to adjust the effect of consistency loss. Note that although we encourage the perturbed images to share a similar style, the adversarial noise is constrained by the attack strength and cannot enforce identical styles across images. Nevertheless, promoting similar styles is beneficial for the protection of privacy.

Dynamic ratio strategy. The ratio λ used to control the impact of consistency loss is dynamically adjusted across PGD [14] iterations. Specifically, suppose the PGD attack runs for a total of K iterations. At the k -th iteration, instead of using a fixed λ , we search for the optimal λ_k from a predefined interval $[0, R]$.

For each candidate ratio $r \in [0, R]$, we calculate the gradient at the k -th iteration with the combined loss \mathcal{L} . This gradient is then used to update Δ , and the resulting perturbed image at the $k + 1$ -th iteration is obtained by adding Δ to the set of clean images \mathcal{X} . We then evaluate the reconstruction loss \mathcal{L}_{re} using this $k + 1$ -th perturbed image. Among all candidate ratios r , we select the one that yields the largest \mathcal{L}_{re} after the update, and assign it as λ_k for the current iteration.

The rationale is that a well-chosen ratio should lead to a perturbation that causes more significant degradation in diffusion-based reconstruction, thereby enhancing the attack’s effectiveness.

Algorithm. The overall procedure of our CAP method is in Algorithm 1. Note that we do not add the consistency loss at the beginning of the attack. Instead, we introduce it at step \hat{k} , after the adversarial noise has preliminarily formed, as adding the style loss at that point leads to more stable optimization.

Table 1. Performance comparison on CelebA-HQ and VGGFace2 datasets.

Method	CelebA-HQ				VGGFace2			
	FDNR↑	ISM↓	SER-FIQ↓	CLIP-IQA↓	FDNR↑	ISM↓	SER-FIQ↓	CLIP-IQA↓
Anti-DB	0.1019	0.4243	0.4980	0.6823	0.4150	0.1860	0.2501	0.5316
Anti-DB+CAP	0.1230	0.4056	0.4897	0.6746	0.4338	0.1841	0.2381	0.5232
SimAC	0.7160	0.1077	0.2142	0.4609	0.6225	0.1449	0.2827	0.4419
SimAC+CAP	0.7446	0.0903	0.2139	0.4525	0.6813	0.1267	0.2679	0.4331

5 Experiment

Dataset. In this study, we utilized two widely used face datasets, CelebA-HQ [9] and VGGFace2 [1], to evaluate the effectiveness of the proposed method, with each dataset containing approximately 50 individuals. For each individual, four images serve as the published image set that need privacy protection. All images were center-cropped and uniformly resized to a resolution of 512×512 .

Baselines. To evaluate the improvements introduced by CAP, we use Anti-DreamBooth [22] and the state-of-the-art SimAC [24] method as baselines. We then integrate the CAP method into each to perform a comparative analysis. Specifically, we assess the protection performance before and after incorporating CAP under identical experimental settings, allowing us to isolate the contribution of our proposed consistency-aware strategy. This setup enables a fair and comprehensive evaluation of CAP’s effectiveness.

Metric. In this paper, to comprehensively evaluate both the protection effectiveness and image quality under defense, we employed four evaluation metrics. We used RetinaFace [2] as the face detector to determine whether a detectable face exists in the generated image, thereby calculating the Face Detection Failure Rate (FDFR). If a face is detected, we encode it using ArcFace [3] and compute the cosine similarity between the encoded feature and the average facial feature vector of the corresponding clean image set, which we refer to as the Identity Score Matching score (ISM). We set the ISM score to zero for images in which no face is detected. Note that FDFR and ISM are the core metrics for evaluating the protection capability of anti-personalization methods. A higher FDFR and lower ISM indicate a better privacy protection effect. To evaluate the quality of the detected face images, we adopted SER-FIQ [21], a face image quality assessment metric. In addition, we computed CLIP-IQA [25] to assess the overall image quality, which is an unsupervised image quality and perceptual assessment method based on the CLIP model.

Implementation details. For all methods, we uniformly set the noise step size α to 0.005 and the adversarial noise strength η to 0.05. Our CAP method introduces the consistency loss into the attack procedure at half of the iteration process. We perform style extraction using VGG-19 by computing Gram matrices from features extracted from the first five convolutional layers. Additionally, we use a DreamBooth model based on Stable Diffusion 2.1, trained with a batch size of 2, a learning rate of 5×10^{-7} , and a total of 1,000 training steps, just following the setting of the Anti-DreamBooth and SimAC. For evaluation, 16 images are generated for each individual. All experiments are performed on a workstation with Ubuntu 22.04.6 LTS and an A800 GPU with 80GB memory.

5.1 Comparison with Baseline

To evaluate the generality and effectiveness of our method in improving the performance of existing anti-personalization approaches, we report the experimental results in Table 1. We conduct experiments on two benchmark datasets, CelebA-HQ and VGGFace2, to evaluate the effectiveness of our proposed CAP method. We apply CAP to two existing anti-personalization baselines, Anti-DreamBooth and SimAC, denoted as “Anti-DB” and “SimAC” in the table. Note that Anti-DB includes two variants, FSMG and ASPL; therefore, we report the average results across both versions. On the CelebA-HQ dataset, Anti-DB+CAP achieves an FDFR of 0.1230, representing a 20% improvement over Anti-DB (0.1019). Similarly, SimAC+CAP achieves 0.7446, exceeding SimAC’s 0.7160 by 3%. For the ISM metric, Anti-DB+CAP reduces the value from 0.4243 to 0.4056 (4% improvement), while SimAC+CAP lowers it from 0.1077 to 0.0903 (16% improvement). Improvements are also observed in the SER-FIQ and CLIP-IQA metrics, indicating enhanced privacy protection without perceptual degradation. On the VGGFace2 dataset, a consistent trend is observed. Anti-DB+CAP achieves an FDFR of 0.4338, a 4% gain over Anti-DB (0.4150), and SimAC+CAP improves FDFR from 0.6225 to 0.6813 (9% increase). In terms



Fig. 3. Visualization. Here, we present the performance of Anti-DB and SimAC, along with the additional improvements achieved by integrating our CAP method.

Table 2. Comparison between style loss and content loss.

Method	FDFR↑	ISM↓
Anti-DB	0.0897	0.4236
Anti-DB+CAP (Content)	0.0951	0.4153
Anti-DB+CAP (Style)	0.1359	0.3938

Table 3. Compare static ratio and dynamic ratio strategy.

Method	FDFR↑	ISM↓
Static_Ratio=20	0.1060	0.4101
Static_Ratio=40	0.1033	0.4062
Static_Ratio=60	0.0924	0.4066
Static_Ratio=80	0.1182	0.4150
Static_Ratio=100	0.0978	0.4100
CAP	0.1359	0.3938

of ISM, Anti-DB+CAP reduces the score from 0.1860 to 0.1841, and SimAC+CAP achieves a 12% reduction, from 0.1449 to 0.1267. Overall, these results demonstrate that our CAP method consistently enhances the performance of existing anti-personalization methods across multiple metrics and datasets, underscoring the importance of incorporating consistency constraints in the design of privacy protection against personalization.

Visualization. The visualization result is shown in Figure 3. we can find that our CAP method can successfully improve the Anti-DB and SimAC method on privacy protection task.

5.2 Ablation Study

To evaluate the effectiveness of the proposed style consistency loss and dynamic ratio strategy, we conduct experiments on the CelebA-HQ dataset using the Anti-DreamBooth (FSMG version).

5.2.1 Style consistency loss. Although incorporating consistency loss into anti-personalization methods is a promising direction, the design of inter-image relationships among perturbed images remains underexplored. In Table 2, we evaluate the effectiveness of applying style consistency loss or content consistency loss [5]. The results show that while content consistency provides a modest improvement over the baseline Anti-DB method, the gain is limited. In contrast, style consistency leads to a significantly greater enhancement, highlighting its stronger impact on the privacy protection task against personalization methods.

5.2.2 Dynamic ratio strategy. In Table 3, we evaluate the effectiveness of the proposed dynamic ratio adjustment strategy. The dynamic ratio in our method is selected within the range of [0, 100]. For comparison, we experiment with several fixed (static) ratios: 20, 40, 60, 80, and 100. As shown in the results, no single static ratio consistently achieves optimal performance across all metrics. For instance, a static ratio of 80 yields the highest FDFR, while a ratio of 40 achieves the lowest ISM. In contrast, our dynamic strategy (CAP) achieves superior performance on both FDFR and ISM, demonstrating its adaptability and overall effectiveness.

Table 4. Using different CNN for style extraction.

Method	FDFR \uparrow	ISM \downarrow
Anti-DB	0.0897	0.4236
Anti-DB+CAP (ResNet50)	0.1128	0.4053
Anti-DB+CAP (VGG19)	0.1359	0.3938

Table 5. Different search ratio range $[0, R]$

Method	FDFR \uparrow	ISM \downarrow
Anti-DB	0.0897	0.4236
Anti-DB+CAP ($R=50$)	0.1087	0.4069
Anti-DB+CAP ($R=100$)	0.1359	0.3938

5.3 Discussion

5.3.1 Different CNN for style extraction. In Table 4, we evaluate the performance of our CAP method using different CNN architectures for style extraction, specifically the classical VGG-19 and ResNet50 [7]. The results show that both architectures effectively enhance the Anti-DB baseline, and using VGG-19 can achieve the best result. The result demonstrates the generalizability of the proposed CAP framework across different backbone networks.

5.3.2 Range of search ratio. In Table 5, we evaluate the effectiveness of our CAP method under different search ratio ranges, specifically $[0, 50]$ and $[0, 100]$. In both settings, Anti-DB+CAP outperforms the baseline Anti-DB, demonstrating the effectiveness of incorporating consistency constraints. Notably, the search ratio range of $[0, 100]$ yields the best overall performance, indicating that a broader search space facilitates more effective optimization.

5.3.3 Different perturbation strength. In Figure 4, we present the protection effects of applying adversarial perturbations to published images under varying perturbation strengths: $\frac{4}{255}$, $\frac{8}{255}$, $\frac{12}{255}$, and $\frac{16}{255}$. The results show that stronger perturbations lead to more effective privacy protection.

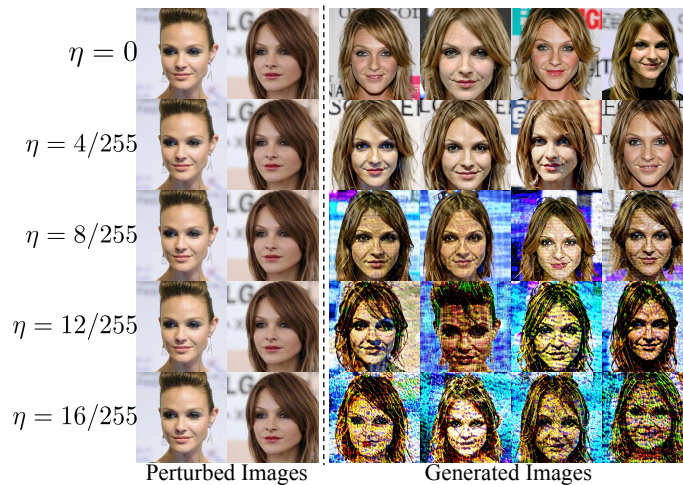


Fig. 4. Privacy Protection effect under different perturbation strength.

6 Conclusion

This paper presents Cross-image Anti-Personalization (CAP), a novel defense framework designed to counter unauthorized personalization in text-to-image diffusion models. Unlike existing methods that apply adversarial noise independently to each image, CAP introduces a style consistency loss that promotes uniformity across perturbed images, thereby leveraging the multi-image nature of personalization tasks. In addition, a dynamic ratio adjustment strategy adaptively balances consistency and reconstruction losses across attack iterations to enhance optimization effectiveness. In future work, we aim to extend the CAP framework to defend against personalization in video or multi-concept scenarios.

References

- [1] Qiong Cao, Li Shen, Weidi Xie, Omkar M Parkhi, and Andrew Zisserman. 2018. Vggface2: A dataset for recognising faces across pose and age. In *2018 13th IEEE international conference on automatic face & gesture recognition (FG 2018)*. IEEE, 67–74.
- [2] Jiankang Deng, Jia Guo, Evangelos Ververas, Irene Kotsia, and Stefanos Zafeiriou. 2020. Retinaface: Single-shot multi-level face localisation in the wild. In *Proceedings of the IEEE/CVF conference on computer vision and pattern recognition*. 5203–5212.
- [3] Jiankang Deng, Jia Guo, Niannan Xue, and Stefanos Zafeiriou. 2019. Arcface: Additive angular margin loss for deep face recognition. In *Proceedings of the IEEE/CVF conference on computer vision and pattern recognition*. 4690–4699.
- [4] Rinon Gal, Yuval Alaluf, Yuval Atzmon, Or Patashnik, Amit Haim Bermano, Gal Chechik, and Daniel Cohen-or. 2023. An Image is Worth One Word: Personalizing Text-to-Image Generation using Textual Inversion. In *The Eleventh International Conference on Learning Representations*. <https://openreview.net/forum?id=NAQvF08TcyG>
- [5] Leon A Gatys, Alexander S Ecker, and Matthias Bethge. 2016. Image style transfer using convolutional neural networks. In *Proceedings of the IEEE conference on computer vision and pattern recognition*. 2414–2423.
- [6] Ian J Goodfellow, Jean Pouget-Abadie, Mehdi Mirza, Bing Xu, David Warde-Farley, Sherjil Ozair, Aaron Courville, and Yoshua Bengio. 2014. Generative adversarial nets. *Advances in neural information processing systems* 27 (2014).
- [7] Kaiming He, Xiangyu Zhang, Shaoqing Ren, and Jian Sun. 2015. Deep Residual Learning for Image Recognition. arXiv:1512.03385 [cs.CV] <https://arxiv.org/abs/1512.03385>
- [8] Jonathan Ho, Ajay Jain, and Pieter Abbeel. 2020. Denoising diffusion probabilistic models. *Advances in Neural Information Processing Systems* 33 (2020), 6840–6851.
- [9] Tero Karras, Timo Aila, Samuli Laine, and Jaakko Lehtinen. 2018. Progressive growing of GANs for improved quality, stability, and variation. In *International Conference on Learning Representations (ICLR)*.
- [10] Diederik P Kingma, Max Welling, et al. 2013. Auto-encoding variational bayes.
- [11] Nupur Kumari, Bingliang Zhang, Richard Zhang, Eli Shechtman, and Jun-Yan Zhu. 2023. Multi-concept customization of text-to-image diffusion. In *Proceedings of the IEEE/CVF conference on computer vision and pattern recognition*. 1931–1941.
- [12] Chumeng Liang and Xiaoyu Wu. 2023. Mist: Towards improved adversarial examples for diffusion models. *arXiv preprint arXiv:2305.12683* (2023).
- [13] Yixin Liu, Chenrui Fan, Yutong Dai, Xun Chen, Pan Zhou, and Lichao Sun. 2024. Metacloak: Preventing unauthorized subject-driven text-to-image diffusion-based synthesis via meta-learning. In *Proceedings of the IEEE/CVF Conference on Computer Vision and Pattern Recognition*. 24219–24228.
- [14] Aleksander Madry, Aleksandar Makelev, Ludwig Schmidt, Dimitris Tsipras, and Adrian Vladu. 2018. Towards Deep Learning Models Resistant to Adversarial Attacks. In *International Conference on Learning Representations*. <https://openreview.net/forum?id=rjzIBfZAb>
- [15] Robin Rombach, Andreas Blattmann, Dominik Lorenz, Patrick Esser, and Björn Ommer. 2022. High-resolution image synthesis with latent diffusion models. In *Proceedings of the IEEE/CVF Conference on Computer Vision and Pattern Recognition*. 10684–10695.
- [16] Nataniel Ruiz, Yuanzhen Li, Varun Jampani, Yael Pritch, Michael Rubinstein, and Kfir Aberman. 2023. Dreambooth: Fine tuning text-to-image diffusion models for subject-driven generation. In *Proceedings of the IEEE/CVF conference on computer vision and pattern recognition*. 22500–22510.
- [17] Christoph Schuhmann, Romain Beaumont, Richard Vencu, Cade Gordon, Ross Wightman, Mehdi Cherti, Theo Coombes, Aarush Katta, Clayton Mullis, Mitchell Wortsman, et al. 2022. Laion-5b: An open large-scale dataset for training next generation image-text models. *Advances in neural information processing systems* 35 (2022), 25278–25294.
- [18] Karen Simonyan and Andrew Zisserman. 2014. Very deep convolutional networks for large-scale image recognition. *arXiv preprint arXiv:1409.1556* (2014).
- [19] Victor Sreeram and P Agathoklis. 1994. On the properties of Gram matrix. *IEEE Transactions on Circuits and Systems I: Fundamental Theory and Applications* 41, 3 (1994), 234–237.
- [20] Stability AI. 2023. Stable Diffusion Version 2. <https://github.com/Stability-AI/stablediffusion> Accessed: 2023-05-01.
- [21] Philipp Terhorst, Jan Niklas Kolf, Naser Damer, Florian Kirchbuchner, and Arjan Kuijper. 2020. SER-FIQ: Unsupervised estimation of face image quality based on stochastic embedding robustness. In *Proceedings of the IEEE/CVF conference on computer vision and pattern recognition*. 5651–5660.

- [22] Thanh Van Le, Hao Phung, Thuan Hoang Nguyen, Quan Dao, Ngoc N Tran, and Anh Tran. 2023. Anti-dreambooth: Protecting users from personalized text-to-image synthesis. In *Proceedings of the IEEE/CVF International Conference on Computer Vision*. 2116–2127.
- [23] Bingyuan Wang, Qifeng Chen, and Zeyu Wang. 2024. Diffusion-based visual art creation: A survey and new perspectives. *arXiv preprint arXiv:2408.12128* (2024).
- [24] Feifei Wang, Zhentao Tan, Tianyi Wei, Yue Wu, and Qidong Huang. 2024. Simac: A simple anti-customization method for protecting face privacy against text-to-image synthesis of diffusion models. In *Proceedings of the IEEE/CVF Conference on Computer Vision and Pattern Recognition*. 12047–12056.
- [25] Jianyi Wang, Kelvin CK Chan, and Chen Change Loy. 2023. Exploring clip for assessing the look and feel of images. In *Proceedings of the AAAI conference on artificial intelligence*, Vol. 37. 2555–2563.
- [26] Xiyu Wang, Yufei Wang, Satoshi Tsutsui, Weisi Lin, Bihan Wen, and Alex Kot. 2024. Evolving storytelling: benchmarks and methods for new character customization with diffusion models. In *Proceedings of the 32nd ACM International Conference on Multimedia*. 3751–3760.
- [27] Jingyuan Yang, Jiawei Feng, and Hui Huang. 2024. EmoGen: Emotional image content generation with text-to-image diffusion models. In *Proceedings of the IEEE/CVF Conference on Computer Vision and Pattern Recognition*. 6358–6368.
- [28] Zhengyue Zhao, Jinhao Duan, Xing Hu, Kaidi Xu, Chenan Wang, Rui Zhang, Zidong Du, Qi Guo, and Yunji Chen. 2023. Unlearnable examples for diffusion models: Protect data from unauthorized exploitation. *arXiv preprint arXiv:2306.01902* (2023).